Materials Transactions, Vol. 59, No. 1 (2018) pp. 88 to 97

Effective Alloying Treatment for Platinum Using Iron Chloride Vapor

Yu-ki Taninouchi* and Toru H. Okabe

Institute of Industrial Science, The University of Tokyo, Tokyo 153–8505, Japan

An effective alloying treatment for Pt using $FeCl_x$ (x = 2, 3) vapor was demonstrated towards developing a novel recovery process for platinum group metals (PGMs) in catalyst scrap. Suitable reaction conditions were discussed from the perspective of thermodynamics, and its validity was confirmed experimentally. When pure Pt samples were reacted with $FeCl_2$ vapor at 1200 K under the coexistence of metallic Fe, an Fe-Pt alloy showing ferromagnetism was easily formed, even though the samples were not in physical contact with the metallic Fe. On the basis of thermodynamic considerations, alloying of Pt mainly proceeds via the disproportionation of $FeCl_2$ vapor, with the gaseous phase containing $FeCl_x$ acting as the medium to transport Fe from the metallic Fe to the Pt samples. When the alloyed sample was kept under $FeCl_3$ vapor at 1200 K, Fe was removed and ferromagnetism was lost. Therefore, it is concluded that $FeCl_2$ vapor treatment under the coexistence of Fe is a feasible and useful technique for alloying Pt and forming a ferromagnetic Fe-Pt alloy. The results obtained in this study indicate that treatment with $FeCl_2$ vapor followed by magnetic separation has potential as an effective technique for concentrating PGMs directly from catalyst scrap. [doi:10.2320/matertrans.M-M2017844]

(Received July 28, 2017; Accepted October 16, 2017; Published November 17, 2017)

Keywords: *platinum, iron chloride, iron-platinum alloy, alloying treatment, recycling, ferromagnetism*

1. Introduction

Pt and other platinum group metals (PGMs) are indispensable in various catalysts owing to their unique catalytic activities with excellent heat and corrosion resistance.[1–3] For example, the catalytic converter in automobiles, a device used for detoxifying automobile emissions, usually contains Pt, Pd, and Rh; in 2015, this application accounted for approximately 40% of the world's consumption of Pt.[4] Pt-based catalysts are also widely used in the petroleum refining industry.

The recovery of PGMs including Pt from spent catalysts has been actively carried out in many countries because they are costly to procure. It is notable that the mineral resources of PGMs are predominately localized in South Africa and Russia,[1–4] and that their extraction and subsequent treatment generates large quantities of waste and consumes a considerable amount of energy. Recycling PGMs is also important for ensuring their steady supply and for reducing the environmental burden.

Most catalyst scrap has a complicated structure, with Pt and other PGMs present as minor components. For example, automobile catalytic converters mostly consist of a honeycomb-structured ceramic substrate composed of cordierite or a similar chemically stable ceramic material. The substrate is coated with a porous catalyst layer consisting of various oxides such as alumina and ceria. PGMs are supported on the porous catalyst layer in the form of fine particles, with the total PGM concentration in the catalyst being approximately 500–5000 mass ppm.[2,5] The low PGM concentrations and the complex scrap structure make the effective recovery of PGMs difficult. Furthermore, PGMs are chemically stable and do not react with most acids. The high chemical stabilities of PGMs also make their extraction difficult.

In typical commercial recycling processes, catalyst scraps are mechanically pulverized in order to evaluate the PGM content (i.e., the scrap value), and then subjected to a pyrometallurgical process to concentrate the PGMs.[2,3] Subsequently, the enriched PGMs are dissolved using strong oxidizing acids, such as aqua regia (HCl/HNO_3) and hydrochloric acid with chlorine gas (HCl/Cl_2).[1–3,6] Finally, the PGMs extracted into HCl solution are purified and separated using various hydrometallurgical techniques such as solvent extraction, precipitation, and ion exchange.[1–3,7] In the pyrometallurgical concentration process, catalyst scraps are smelted with a collector metal such as Cu or Fe; the PGMs are concentrated in the metallic phase, and the ceramic components of the scraps are removed as slag waste.[1–3,8,9] While the pyrometallurgical process is an effective upgrading technique for catalyst scraps, it requires large-scale equipment and is energy-intensive.

In general, physical separation such as flotation and magnetic separation can be performed using simple and small-scale equipment with low energy consumption. Thus, some studies have been conducted on the enrichment process based on physical separation techniques. For example, magnetic separation after pulverization,[10,11] flotation after pulverization,[11,12] selective grinding followed by size separation,[13,14] and selective grinding after a heating/quenching treatment[15] have been investigated for physically concentrating PGMs from spent automobile catalysts. Furthermore, physical concentration techniques involving chemical pretreatments, such as alloying, sulfurization, and electroless plating, have also been explored.[16–20] However, these techniques are still in the research stage or are not practical for industrial use. Nevertheless, they have potential for reducing the energy consumption and environmental burden of the existing recycling process. Furthermore, if a physical concentration pretreatment could sufficiently enrich the PGMs, they could be effectively extracted by acid dissolution without employing the pyrometallurgical concentration process.

In order to develop a novel physical concentration technique where the PGMs are efficiently concentrated by mag-

*Corresponding author, E-mail: taninou@iis.u-tokyo.ac.jp. Present address: Department of Materials Science and Engineering, Kyoto University, Kyoto 606–8501, Japan

netic separation, the present authors have focused on the vapor-based alloying pretreatment for PGMs shown in Fig. 1. To the best of our knowledge, Okabe and Mitsui first proposed in a patent the basic concept of magnetic concentration involving alloying pretreatment.[16] Notably, some of the alloys between Fe and PGMs show strong ferromagnetism close to room temperature. In addition, alloying with Fe can facilitate the acid dissolution of the PGMs.[21] Thus, alloying with Fe is a valuable pretreatment for magnetically concentrating the PGMs from catalyst scrap. However, because PGMs are present on the scrap surface, which is inherently complex, it is quite difficult to alloy them directly by the reaction with solid Fe. Thus, in the alloying and magnetizing treatment shown in Fig. 1, $FeCl_x$ (x = 2, 3) vapor is used as the reactant. As shown in Fig. 2, $FeCl_2$ and $FeCl_3$ are highly volatile compared with Fe.[22] This means that $FeCl_x$ vapor can be easily and effectively supplied to the PGMs on the scrap surfaces by heating.

Although alloying pretreatment using $FeCl_x$ vapor is attractive for the reasons given above, research on this technique is quite limited. In the patent by Okabe and Mitsui, for example, powder PGM samples (Pt, Pd, and Rh) were alloyed with Fe when heated under $FeCl_3$ vapor at 973–1273 K in a quartz chamber.[16] However, the reported results included large uncertainties and were not reproducible. In our previous study,[20] alloying and magnetization of PGMs (Pt, Pd, and Rh) was confirmed when thin wire samples were reacted with $FeCl_2$ vapor in a steel vessel maintained at 1200 K. However, the research was preliminary, and the alloying reaction mechanism was unclear. In this study, thermodynamic analyses and experiments were conducted on the $FeCl_x$-vapor-based alloying treatment for Pt and the reaction system that effectively alloys Pt with Fe is clarified.

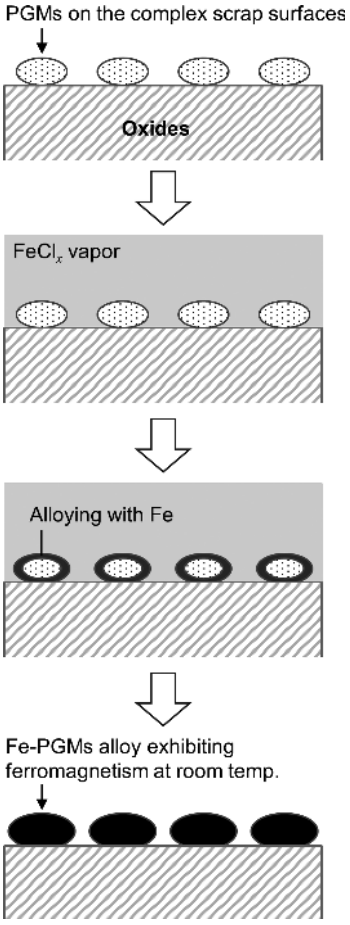

Fig. 1 Schematic illustration of alloying treatment using $FeCl_x$ (x = 2, 3) vapor. After the alloying treatment, PGMs can be effectively concentrated by magnetic separation.

2. Thermodynamic Considerations

Alloying treatment of Pt is discussed at a reaction temperature of 1200 K. At this temperature, the stable phase of $FeCl_2$ is liquid. However, its vapor pressure (p_{FeCl_2}) is as high as 3.2×10^{-1} atm,[22] as shown in Fig. 2, and it is possible to effectively supply $FeCl_2$ vapor on Pt. $FeCl_3$ is more volatile than $FeCl_2$. $FeCl_3$ volatilizes mainly as a dimer at relatively low temperatures, but its monomeric gas becomes stable near 1200 K. It is also noteworthy that analogous preliminary experiments were performed at around this temperature in previous studies.[16,20]

Figure 3(a) shows the phase diagram of the Fe-Pt system.[23–25] Pure Pt has a face-centered cubic (fcc) structure and forms a fcc solid solution (γ-(Fe,Pt)) with Fe. Besides a disordered fcc phase, three stable ordered phases are present (i.e., γ_1-Fe_3Pt with an $L1_2$ structure, γ_2-FePt with an $L1_0$ structure, and γ_3-$FePt_3$ with an $L1_2$ structure). In addition, a stable region of the solid solution with a body-centered cubic (bcc) structure (α-(Fe,Pt)) is present at the Fe-rich region below 1185 K. α-(Fe,Pt), γ_1-Fe_3Pt, and γ_2-FePt exhibit ferromagnetism at ordinary temperatures (~298 K).

As shown in Fig. 3(a), with an increase in the Fe concentration at 1200 K, the stable phase changes from Pt-rich γ-(Fe,Pt) to γ_3-$FePt_3$, to γ_2-FePt, and then to Fe-rich γ-(Fe,Pt). The reported phase boundaries relating to the ordered phases differ somewhat in the literature.[23,24,26–28] However, Fig. 3(a) shows that γ_2-FePt or Fe-Pt alloys con-

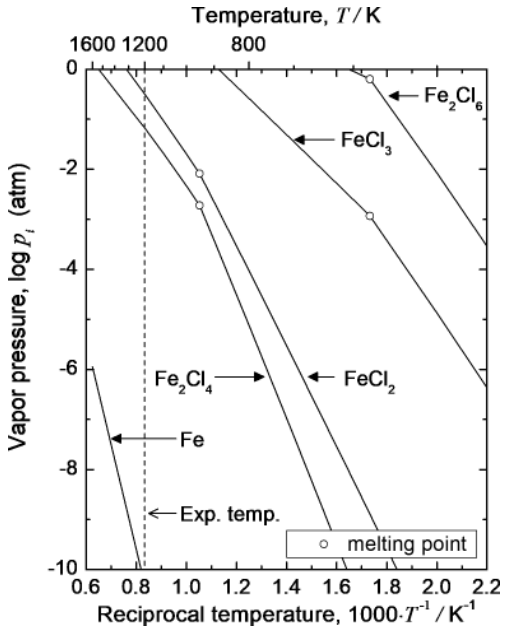

Fig. 2 Vapor pressures of Fe and its chlorides. Thermodynamic data in reference[22] was used. Open circles indicate the melting points.

taining γ_2-FePt (i.e., a mixture of γ_3-$FePt_3$ and γ_2-FePt and a mixture of γ_2-FePt and Fe-rich γ-(Fe,Pt)) become stable at an Fe concentration of approximately 35–65 mol%. γ_2-FePt is ferromagnetic at room temperature, and its formation allows us to effectively recover the Pt from scrap by magnetic separation. When the Fe concentration exceeds approximately 65 mol% at 1200 K, the Fe-rich γ-(Fe,Pt) phase becomes stable. This Fe-rich phase can be converted into Fe-Pt alloys with ferromagnetic properties at room temperature (i.e., α-(Fe,Pt), γ_1-Fe_3Pt, and/or γ_2-FePt) during cooling or by annealing at intermediate temperatures. For the efficient recovery of Pt from catalyst scraps by magnetic separation, it is necessary to convert Pt into γ_2-FePt and/or Fe-rich γ-(Fe,Pt) in the alloying reaction at 1200 K.

Fredriksson and Seetharaman measured the activities of Fe (a_{Fe}) in some Fe-Pt alloys (their compositions are denoted by open circles in Fig. 3(a)) by the solid-electrolyte galvanic cell method in the temperature range of 1073–1273 K.[25] Base on this study, a_{Fe} was evaluated at 1200 K and shown in Fig. 3(b). In the evaluation of a_{Fe}, the standard state of Fe was defined to be its pure solid state. Overall, the a_{Fe} values show negative deviation from ideality due to the strong affinity of Fe with Pt. The a_{Fe} value under the γ-(Fe,Pt)/γ_2-FePt equilibrium was estimated to be ~5×10^{-1}, based on the a_{Fe} values of points b and c. Meanwhile, the a_{Fe} value under the γ_2-FePt/γ_3-$FePt_3$ equilibrium was 4×10^{-2}, as represented by the a_{Fe} values of point d. In terms of equilibrium, Pt can be converted into γ_2-FePt when the a_{Fe} of the reaction system is higher than 4×10^{-2}. Furthermore, when the a_{Fe} of the reaction system is higher than ~5×10^{-1}, Fe-rich γ-(Fe,Pt) can form at 1200 K.

Figure 4 shows the chemical potential diagram for the Fe-Cl-O system. The diagram was calculated at 1200 K using thermodynamic data[22] based on the assumption that the activity of all chemical species is unity (the standard state of gaseous species is 1 atm). The axes correspond to the logarithms of a_{Fe}, the partial pressure of chlorine (p_{Cl_2}), and the partial pressure of oxygen (p_{O_2}). The most stable phases are represented as faces, whereas the phase equilibria are indicated by the intersections between these faces.

Figure 4 shows that $FeCl_2(l)$ equilibrates with Fe(s) and FeO(s) at the potential point α: $a_{Fe} = 1$, $p_{Cl_2} = 1 \times 10^{-9}$ atm, and $p_{O_2} = 1 \times 10^{-17}$ atm. This indicates that when the amounts of Fe(s) and $FeCl_2(l)$ are present in sufficient quantities in the reaction system, its chemical potential can be maintained close to point α (i.e., a high a_{Fe} condition). From the viewpoint of equilibrium, alloying Pt with Fe proceeds until the a_{Fe} of the Fe-Pt alloy equals the a_{Fe} of the reaction system. As mentioned earlier, $FeCl_2(l)$ equilibrates with $FeCl_2(g)$ with a partial pressure of 3.2×10^{-1} atm at 1200 K. Therefore, the reaction with $FeCl_2$ vapor under the coexistence with Fe(s) and $FeCl_2(l)$ has the potential to convert Pt into γ_2-FePt and/or Fe-rich γ-(Fe,Pt).

Figure 4 also indicates that $FeCl_3(g)$ is stable under low a_{Fe} and high p_{Cl_2} conditions. $FeCl_3(g)$ cannot coexist with Fe(s) and equilibrates with $FeCl_2(l)$ and $Fe_2O_3(s)$ at the potential point β: $a_{Fe} = 1 \times 10^{-7}$, $p_{Cl_2} = 1 \times 10^{-2}$ atm, and $p_{O_2} = 3 \times 10^{-6}$ atm. The a_{Fe} region where $FeCl_3(g)$ is stable is much lower than the a_{Fe} in γ_2-FePt (a_{Fe}) and Fe-rich γ-(Fe,Pt). This means that Pt cannot be converted into γ_2-FePt and/or Fe-rich γ-(Fe,Pt) by reacting with $FeCl_3$ vapor

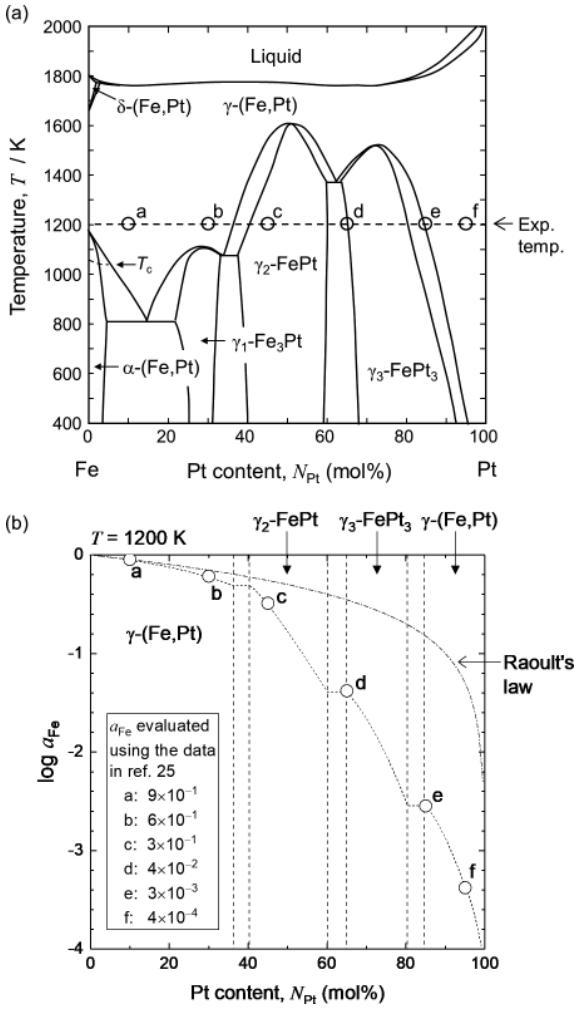

Fig. 3 (a) Phase diagram for the Fe-Pt system[23,24] and (b) activities of Fe estimated at 1200 K. The Fe activities at the composition and temperature denoted by open circles were evaluated based on the reported data.[25]

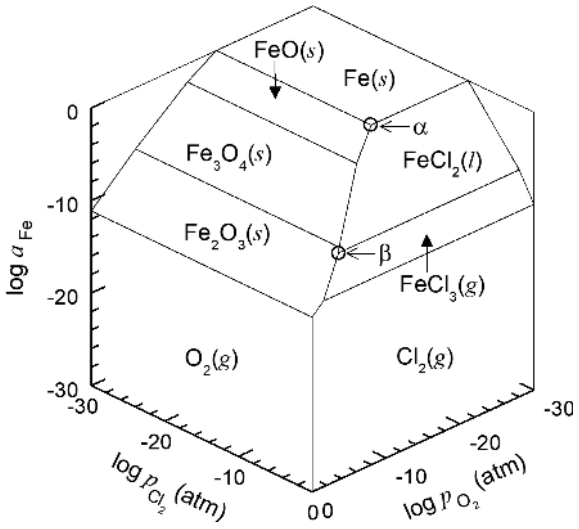

Fig. 4 Chemical potential diagram for the Fe-Cl-O system at 1200 K. Thermodynamic data in reference[22] was used. The potential point α and β corresponds to the Fe/$FeCl_2$/FeO and $FeCl_2$/$FeCl_3$/Fe_2O_3 equilibria, respectively.

at 1200 K. In other words, if the γ_2-FePt or Fe-rich γ-(Fe,Pt) is kept under $FeCl_3$ vapor, dealloying would proceed as follows:

$$Fe(s, \text{in Pt}) + 2FeCl_3(g) \rightarrow 3FeCl_2(l) \quad (1)$$

$$Fe(s) + 2FeCl_3(g) = 3FeCl_2(l) \quad (2)$$

$$\Delta G^\circ_{(2)} = -160\,\text{kJ at } 1200\,\text{K},^{22)}$$

where $\Delta G^\circ_{(2)}$ is the standard Gibbs energy of reaction (2).

When Pt is reacted with $FeCl_2$ vapor under the coexistence of Fe, two types of alloying reactions can be expected. One of them is a disproportionation of $FeCl_2$ vapor. As shown in Fig. 5(a), when the disproportionation of $FeCl_2$ vapor proceeds on the surface of Pt, Pt is alloyed with Fe, and $FeCl_3$ vapor is generated as a by-product.

$$3FeCl_2(g) \rightarrow Fe(s, \text{ in Pt}) + 2FeCl_3(g) \quad (3)$$

$$3FeCl_2(g) = Fe(s) + 2FeCl_3(g) \quad (4)$$

$$\Delta G^\circ_{(4)} = 126\,\text{kJ at } 1200\,\text{K}^{22)}$$

The $FeCl_3$ generated by the disproportionation diffuses in the gas phase and then reacts with Fe, which regenerates $FeCl_2$.

$$Fe(s) + 2FeCl_3(g) \rightarrow 3FeCl_2(g) \quad (5)$$

Another alloying reaction expected to proceed is the thermal decomposition of $FeCl_2$ vapor, as shown in Fig. 5(b). In this case, Cl_2 gas is generated as a by-product of the alloying reaction.

$$FeCl_2(g) \rightarrow Fe(s, \text{ in Pt}) + Cl_2(g) \quad (6)$$

$$FeCl_2(g) = Fe(s) + Cl_2(g) \quad (7)$$

$$\Delta G^\circ_{(7)} = 194\,\text{kJ at } 1200\,\text{K}^{22)}$$

Subsequently, the Cl_2 gas generated by the thermal decomposition regenerates $FeCl_2$ by reacting with metallic Fe.

$$Fe(s) + Cl_2(g) \rightarrow FeCl_2(g) \quad (8)$$

In either case, $FeCl_2$ vapor acts as a transport medium for Fe and is not consumed in the overall reaction:

$$Fe(s) \rightarrow Fe(s, \text{ in Pt}). \quad (9)$$

Given the dominant alloying reaction in the $FeCl_2$ vapor treatment between disproportionation (reaction (3)) and thermal decomposition (reaction (6)), the equilibrium partial pressures of $FeCl_3$ and Cl_2 (p_{FeCl_3} and p_{Cl_2}, respectively) on the Fe-Pt alloy were calculated at 1200 K using thermodynamic data.[22)] Figure 6 shows the a_{Fe} dependence of the p_{FeCl_3} and p_{Cl_2} when the p_{FeCl_2} is 3.2×10^{-1} atm. The p_{FeCl_3} and p_{Cl_2} equilibrating with the Fe-Pt alloy and $FeCl_2$ vapor decrease with an increase in a_{Fe}. As shown in Fig. 6, the p_{FeCl_3} is orders of magnitude greater than the p_{Cl_2}. For example, when the a_{Fe} is 1×10^{-1} (γ_2-FePt is stable), the p_{FeCl_3} is 1×10^{-3} atm, but the p_{Cl_2} is as low as 1×10^{-8} atm. Thus, it

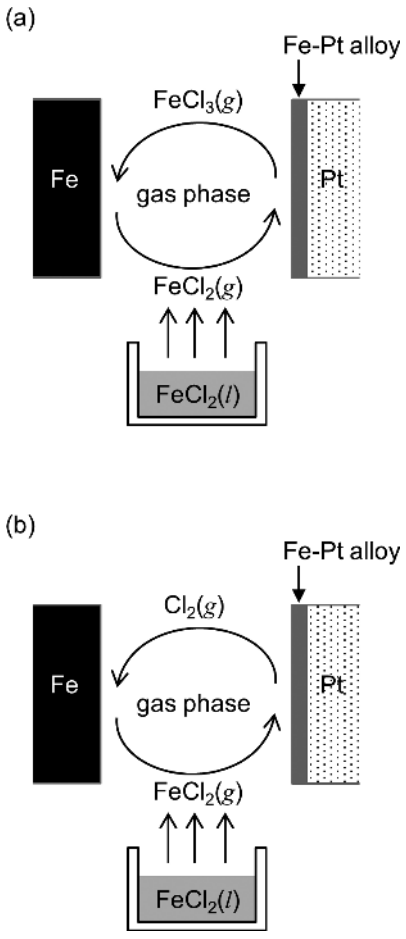

Fig. 5 Schematic illustration of the expected alloying mechanism when Pt is kept in $FeCl_2$ vapor close to 1200 K under the coexistence of metallic Fe. Pt is alloyed with Fe by (a) disproportionation and (b) thermal decomposition of $FeCl_2$ vapor. In either case, the alloying reaction byproduct is converted to $FeCl_2$ by reacting with Fe, and the gas phase acts as a transport medium for Fe.

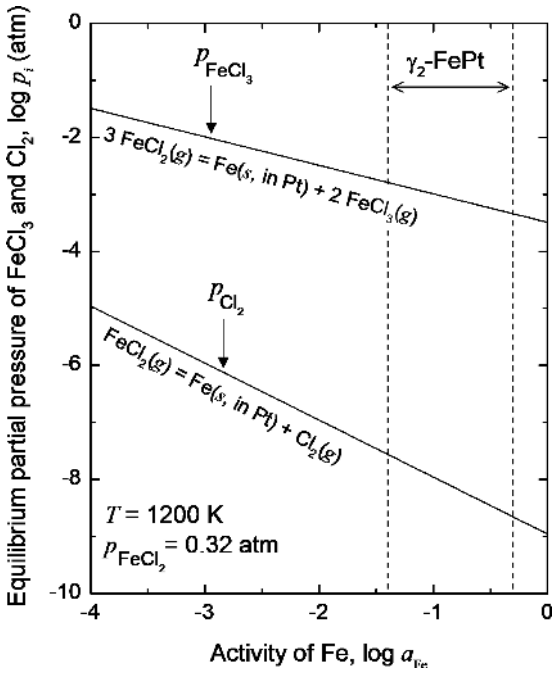

Fig. 6 Equilibrium partial pressures of $FeCl_3$ and Cl_2 on Fe-Pt alloy under $FeCl_2$ vapor at 1200 K. Thermodynamic data in reference[22)] was used.

is reasonable to consider that the alloying of Pt by the thermal decomposition of $FeCl_2$ is negligible. In the proposed $FeCl_2$ vapor treatment (see Fig. 5), alloying of Pt with Fe should proceed mainly by the disproportionation of $FeCl_2$ vapor.

3. Experimental

3.1 Reaction with $FeCl_2$ vapor under the coexistence of Fe

Alloying of Pt using $FeCl_2$ vapor was demonstrated using the experimental apparatus shown in Fig. 7 (Exp. no. 170201_Fe-PGM_exp1). The quartz container, which is composed of four L-shaped units welded to the center unit, was used as the reaction chamber. The four L-shaped units contained either micron-sized Pt powder (99.95%; gray color; Tanaka Kikinzoku Kogyo K.K.; cf. Figure 10(a)) or thin Pt wire (99.99%; diameter (ϕ) = 0.5 mm; length (l) = approximately 20 mm; Tanaka Kikinzoku Kogyo K.K.); their abbreviations and masses of Pt samples are listed in Table 1. A mixture of Fe powder (4.01 g; >95%; Wako Pure Chemical Industries, Ltd.) and $FeCl_2$ powder (0.51 g; 99.9%; Kojundo Chemical Laboratory Co., Ltd.) was placed at the bottom of the center unit. To avoid the adsorption of water from ambient air, a mixture of Fe and $FeCl_2$ powders were loaded in the quartz chamber inside a glove box under a high-purity N_2 atmosphere. The chamber was then sealed in vacuum. The internal volume of the quartz ampoule was approximately 23 mL. In the quartz ampoule, the Pt samples were not in physical contact with the metallic Fe.

The quartz ampoule shown in Fig. 7(b) was kept for 1 h in an electric furnace preheated at 1200 K. After the heat treatment, the ampoule was removed from the furnace and cooled in water. Fig. 7(c) shows the quartz ampoule after the heat treatment. Processed Pt samples were recovered by breaking the ampoule using a hammer. When the quartz ampoule was broken, Pt samples in the form of powder were scattered, and only a fraction of the samples was recovered. The recovered Pt samples were rinsed with distilled water, ethanol, and then acetone before they were dried in air.

After the $FeCl_2$ vapor treatment, the magnetic properties of the powder and wire samples were verified using a small round neodymium magnet (Nd-Fe-B alloy; diameter, ϕ = 7 mm; height, h = 5 mm). For the powder samples, the microstructures and crystalline phases were analyzed by scanning electron microscopy (SEM) using a JSM-6510LV (JEOL) system and by X-ray diffraction (XRD) using a D2 PHASER (Bruker Corporation, Cu-Kα radiation), respectively. Furthermore, the average compositions of the processed powder samples were determined by inductively coupled plasma-atomic emission spectrometry (ICP-AES). For these experiments, a fraction of the powder sample (approximately 0.1 g) was dissolved completely using aqua regia at approximately 333 K. After the solution had evaporated completely, the resulting salt was dissolved again in 50 mL of 2 M HCl. Then, the solution was diluted by 50 times using 2 M HCl to prepare the sample solution. The Fe and Pt concentrations in the sample solution were analyzed using a SPS3520UV (SII NanoTechnology Inc.).

Regarding the wire samples after processing, one of them (Pt-W-1) was subjected to cross-sectional observation. The wire sample was embedded in resin, and SEM and energy-dispersive X-ray spectroscopy (EDS) using a JSM-6510LV (JEOL) were used to analyze the microstructure and composition of the cross-section. Another wire sample (Pt-W-2) was used as a feed material in the experiment described in Section 3.2.

3.2 Reaction with $FeCl_3$ vapor under the coexistence of $FeCl_2$

The instability of Fe-Pt alloy under $FeCl_3$ vapor was confirmed experimentally using the apparatus shown in Fig. 8 (Exp. no. 170213_Fe-PGM_exp4). The Pt wire (Pt-W-2) after alloying treatment using $FeCl_2$ vapor (cf. Section 3.1) was held in a quartz ampoule with a mixture of $FeCl_2$ powder (0.15 g; 99.9%; Kojundo Chemical Laboratory Co., Ltd.), $FeCl_3$ powder (0.026 g; 99%; Kojundo Chemical Laboratory Co., Ltd.), and Fe_2O_3 powder (0.15 g; >95%; Kanto Chemical Co., Ltd.). The internal volume of the quartz ampoule was approximately 22 mL. Since iron chlorides are hydroscopic, the $FeCl_2/FeCl_3/Fe_2O_3$ mixture was treated and loaded in the quartz chamber inside a glove box under a high-purity N_2 atmosphere. Furthermore, the chamber was sealed in vacuum immediately after its removal from the glove box.

The quartz ampoule containing the samples was heated to 1200 K at a heating rate of 1.8 $K \cdot min^{-1}$ in an electric furnace and then maintained at 1200 K for 4 h. After the heat treatment, the ampoule was removed from the furnace and cooled in water. Figures 8(b) and 8(c) show the quartz ampoule before and after the heat treatment, respectively. The wire sample was recovered by breaking the quartz ampoule, and its surface was then rinsed with ethanol. The magnetic property of the wire sample was tested using a handheld neodymium magnet, and cross-sectional SEM/EDS analyses were performed.

4. Results and Discussion

4.1 Alloying of Pt by the reaction with $FeCl_2$ vapor

After the reaction with $FeCl_2$ vapor at 1200 K for 1 h in the quartz ampoule, the resultant powder samples (Pt-P-1 and Pt-P-2) were attached to a magnet, as shown in Figs. 9(a) and 9(b), respectively, and metallic Fe remained at the bottom of the center unit (see Fig. 7(c)). Figure 10 shows the SEM images of the Pt-P-1 powder sample before and after the experiment. The particle size of Pt increased somewhat following the $FeCl_2$ vapor treatment. Figure 11 shows the XRD patterns of the powder samples. It is clear that Pt was effectively alloyed with Fe and that γ_2-FePt, which exhibits ferromagnetism at room temperature, was formed. In the case of Pt-P-1, all diffraction peaks can be rationalized in terms of γ_2-FePt. However, Pt-P-2 contained a small amount of γ_3-$FePt_3$ as a secondary phase. The results of ICP-AES of the obtained powder samples are listed in Table 1. The average compositions of Pt-P-1 and Pt-P-2 were $Fe_{0.46}Pt_{0.54}$ and $Fe_{0.40}Pt_{0.60}$, respectively. In the binary phase diagram shown in Fig. 3, the average composition of Pt-P-1 occurs at the single-phase region of γ_2-FePt. Meanwhile, that of Pt-P-2 occurs near the boundary between

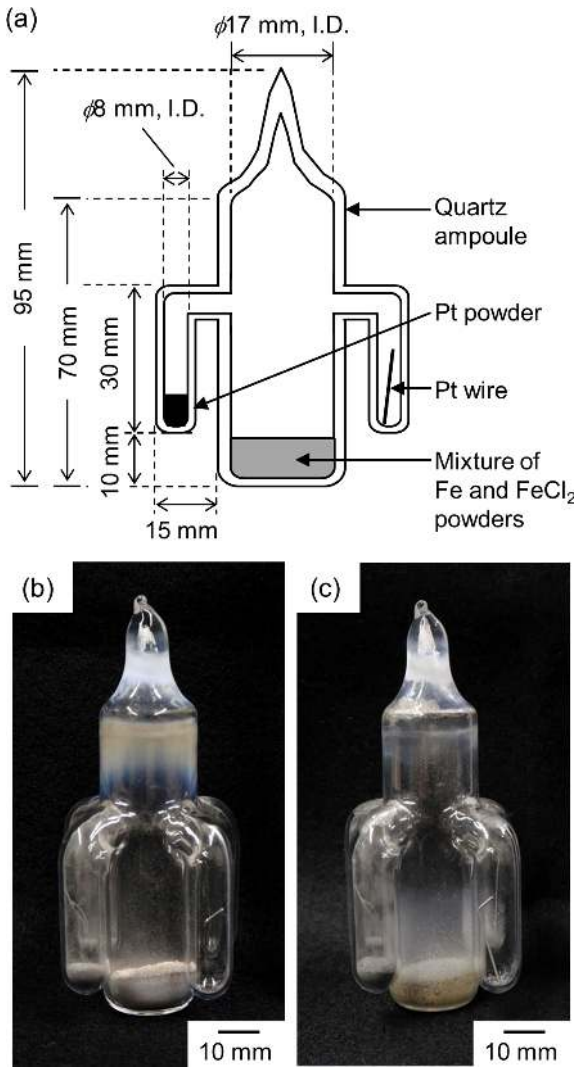

Fig. 7 (a) Schematic illustration of the vacuum-sealed quartz ampoule used for the reaction between Pt and $FeCl_2$ vapor (Exp. no. 170201_Fe-PGM_exp1). Pure Pt samples were placed in the L-shaped unit and did not physically contact the Fe and $FeCl_2$ powder mixture. Photographs of the quartz ampoule (b) before and (c) after the heat treatment at 1200 K for 1 h.

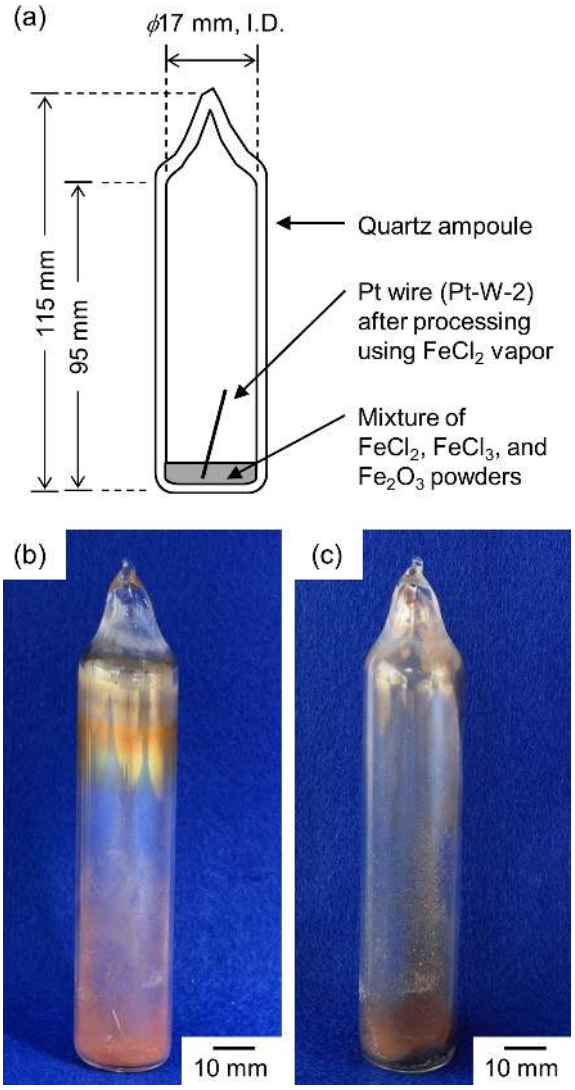

Fig. 8 (a) Schematic illustration of the vacuum-sealed quartz ampoule used for the reaction with $FeCl_3$ vapor (Exp. no. 170213_Fe-PGM_exp4). Photographs of the quartz ampoule (b) before and (c) after heat treatment at 1200 K for 4 h. The processed sample was the Pt wire (Pt-W-2) whose surface was alloyed with Fe by the reaction with $FeCl_2$ vapor (cf. Fig. 9(c)).

Table 1 Abbreviations and masses of pure Pt samples reacted with $FeCl_2$ vapor at 1200 K for 1 h. Average compositions of the powder samples after processing are also summarized.

Exp. no.	Processed Pt sample			Mass of sample after exp., w_{after}/g	Results of ICP-AES			
	Name	Form	Mass, w_{int}/g		Mass conc. of element i, C_i (mass%)		Molar conc. of element i, N_i (mol%)	
					Fe	Pt	Fe [d]	Pt [e]
170201_Fe-PGM_exp1	Pt-P-1	Powder [a]	0.372	(0.42)[c]	19.8	81.1	46	54
	Pt-P-2		0.876	(0.58)[c]	16.5	85.0	40	60
	Pt-W-1	Wire [b]	0.0890	0.0906	–	–	–	–
	Pt-W-2		0.0851	0.0861	–	–	–	–

a: 99.95%; micron-sized as shown in Fig. 10(a).
b: 99.99%; $\phi = 0.5$ mm; $l = \sim 20$ mm.
c: Due to experimental difficulties, not all of the processed samples were recovered.
d: $N_{Fe} = 100 \cdot (C_{Fe}/55.85)/(C_{Fe}/55.85 + C_{Pt}/195.1)$.
e: $N_{Pt} = 100 \cdot (C_{Pt}/195.1)/(C_{Fe}/55.85 + C_{Pt}/195.1)$.

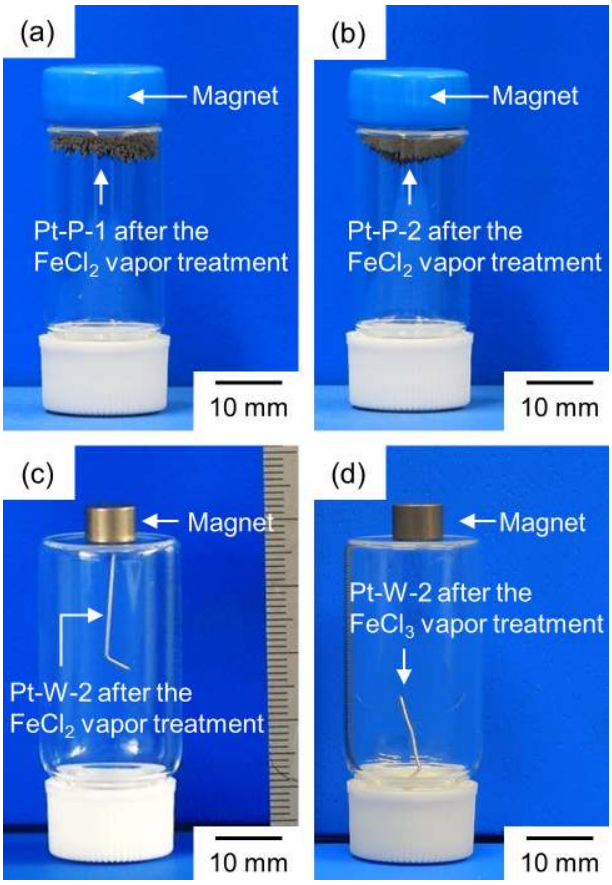

Fig. 9 Photographs of Pt samples after the experiment. (a), (b) powder sample and (c) wire samples after the $FeCl_2$ vapor treatment at 1200 K for 1 h (Exp. no. 170201_Fe-PGM_exp1). Pt samples were attached to a magnet. (d) Pt wire after the $FeCl_3$ vapor treatment at 1200 K for 4 h (Exp. no. 170213_Fe-PGM_exp4). The wire sample did not attach to the magnet after the $FeCl_3$ vapor treatment.

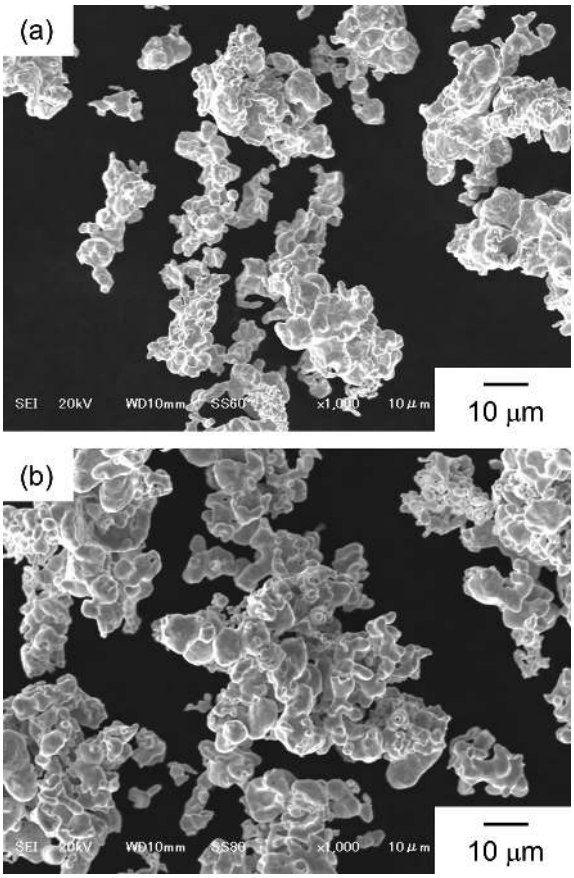

Fig. 10 SEM image of Pt powder (a) before and (b) after the $FeCl_2$ vapor treatment at 1200 K for 1 h (Exp. no. 170201_Fe-PGM_exp1). Pt-P-1 was the sample analyzed.

the γ_2-FePt/γ_3-$FePt_3$ binary-phase region and the γ_2-FePt single-phase region. The average compositions determined by ICP-AES are consistent with the XRD results. The small difference in the alloying behavior between Pt-P-1 and Pt-P-2 is probably related to the difference in weight between the processed samples.

After the experiment, the wire samples (Pt-W-1 and Pt-W-2) also became magnetized, as shown in Fig. 9(c). As reported in Table 1, the masses of the wire samples increased by several percent. Figure 12 shows the results of SEM/EDS for the Pt-W-1 cross-section after the reaction. The area from the surface to a depth of approximately 15 μm was alloyed with Fe. The Fe concentration was approximately 80 mol% at the outermost surface and decreased as the depth increased. The Fe concentration in the near-surface area was high enough to form γ_2-FePt.

The experimental results clearly show that the reaction with $FeCl_2$ vapor at 1200 K under the coexistence of Fe is an effective technique for alloying Pt and forming a ferromagnetic Fe-Pt alloy. Sufficient amounts of Fe and $FeCl_2$ were present in the quartz ampoule. Thus, the chemical potential in the reaction system is close to the potential point α shown in Fig. 4. In this study, the reaction time was only 1 h. Nevertheless, the Pt samples were sufficiently alloyed with

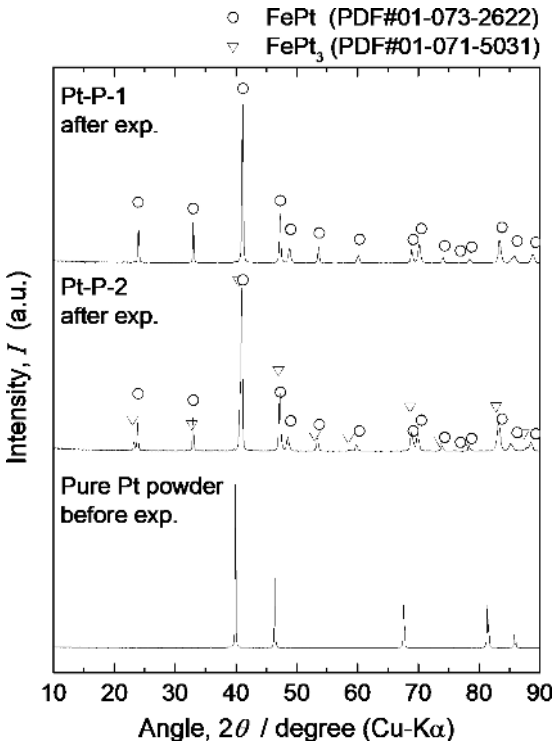

Fig. 11 XRD patterns of Pt samples after the $FeCl_2$ vapor treatment at 1200 K for 1 h (Exp. no. 170201_Fe-PGM_exp1). For reference, the XRD pattern of pure Pt powder before processing is also shown.

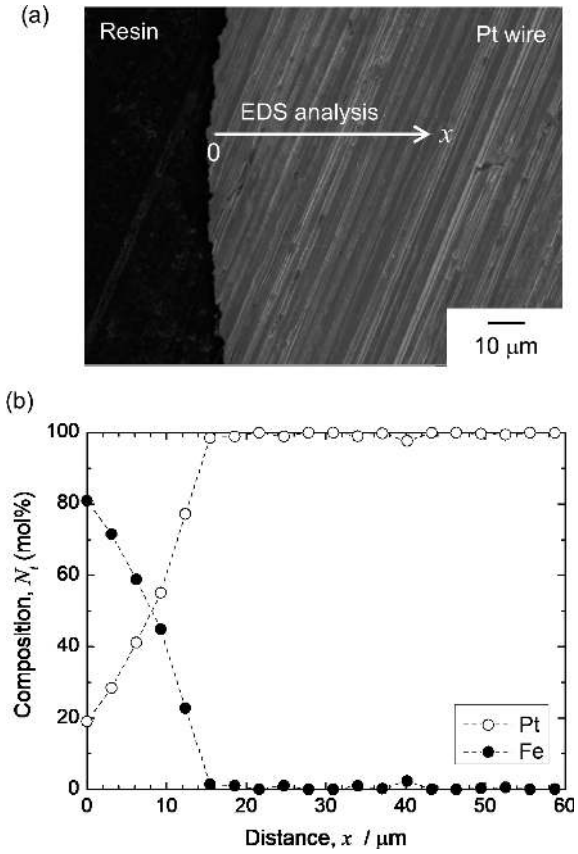

Fig. 12 (a) SEM image and (b) composition profile of a cross section of Pt-W-1 after the $FeCl_2$ vapor treatment at 1200 K for 1 h (Exp. no. 170201_Fe-PGM_exp1).

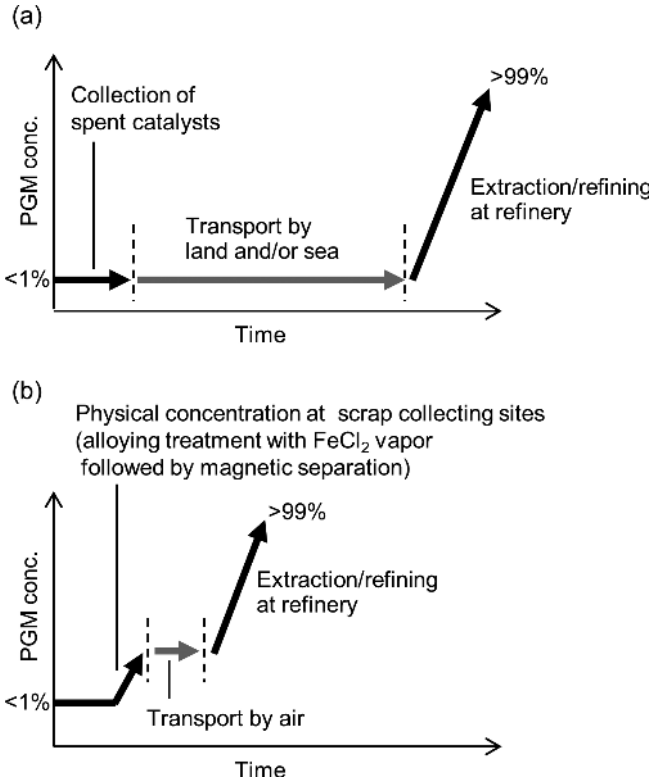

Fig. 13 Schematic illustration of material flow from the collection of spent catalyst to the recovery of refined PGMs. (a) Conventional and (b) new recycling route. In the new recycling route, PGMs are enriched at scrap collecting sites based on the magnetic concentration technique utilizing the alloying pretreatment investigated in this study. Then, the obtained PGM concentrate, which is highly valuable and has a significantly lower volume than untreated scrap, is transported by air for further treatment at a refinery.

Fe to exhibit ferromagnetism. As discussed in Section 3, the alloying of Pt samples can be understood in terms of the disproportionation of $FeCl_2$ vapor and the ability of gaseous phase to serve as an effective transport medium for Fe (see Figs. 5 and 6).

The proposed $FeCl_2$ vapor treatment followed by magnetic separation has potential as a novel process that can effectively concentrate PGMs directly from catalyst scrap. It is expected that other PGMs, such as Pd and Rh, can also be alloyed and magnetized by the reaction with $FeCl_2$ vapor demonstrated in this study. In order to develop this recycling process further, the applicability of the treatment process to other PGMs and the reactivity of the ceramic components in catalyst scraps (e.g., cordierite and alumina) during the vapor treatment must be considered in future studies.

In principle, magnetic concentration using the proposed alloying pretreatment does not require a large-scale plant or a long processing time. Thus, if this recycling process is well developed and put to practical use, the material flow of PGM recycling can be changed as shown in Fig. 13. Catalyst scraps containing Pt and other PGMs, such as spent automobile catalysts, are generated and collected all over the world; they are often transported to refinery by ships and/or by ground transportation methods for extracting and refining PGMs. The proposed magnetic concentration process can be carried out at scrap collecting sites. If the proposed method is adopted for concentrating PGMs, the obtained PGM concentrate, which is highly valuable and has a significantly lower volume than untreated scrap, can be transported by air to refineries for further treatment. In this new recycling route, refined PGMs can be obtained quickly.

4.2 Dealloying of Fe-Pt alloy by the reaction with $FeCl_3$ vapor

The Pt wire (Pt-W-2) whose surface was significantly alloyed with Fe (see Fig. 9(c) and 12) was placed in a quartz ampoule with a mixture of $FeCl_2$, $FeCl_3$, and Fe_2O_3, as shown in Fig. 8, and then heated at 1200 K for 4 h. After the heat treatment, Pt-W-2 did not attach to a magnet, as shown in Fig. 9(d). Furthermore, the weight of Pt-W-2 decreased from 0.0861 g to 0.0852 g during the heat treatment. The sample weight after the heat treatment coincides with that before the alloying treatment using $FeCl_2$ vapor (i.e., the initial weight of Pt-W-2 listed in Table 1). Fig. 14 shows the microstructure and composition profile of a Pt-W-2 cross-section after the experiment. The Fe concentration in the surface area was <10 mol%. Clearly, Fe was removed from the Pt wire during the heat treatment.

During the heat treatment, the wire sample was surrounded by $FeCl_2/FeCl_3$ vapor, and it is reasonable to consider that the chemical potential of the reaction system was maintained close to the potential point β shown in Fig. 4. The dealloying of the Fe-Pt alloy can be explained by its reaction with $FeCl_3$ vapor (i.e., reaction (1)). As predicted on

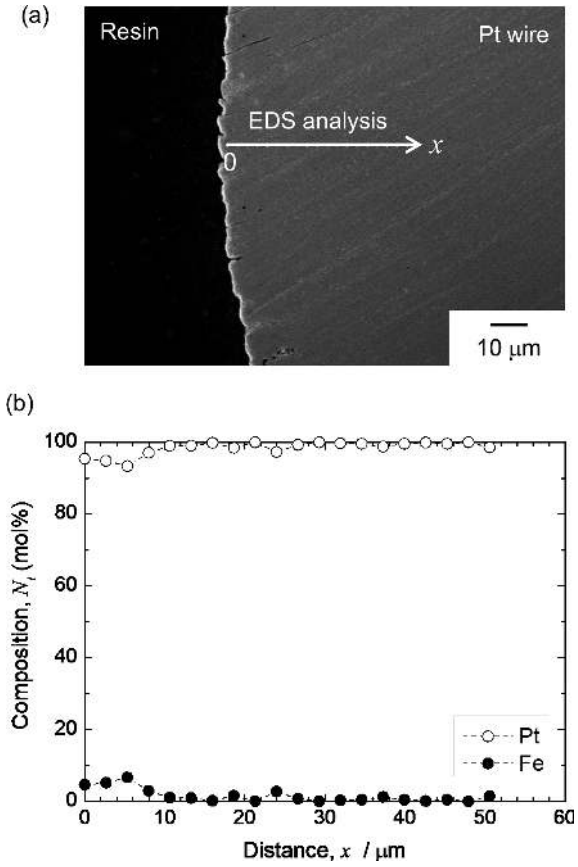

Fig. 14 (a) SEM image and (b) composition profile of a cross section of Pt-W-2 after the $FeCl_3$ vapor treatment at 1200 K for 4 h (Exp. no. 170213_Fe-PGM_exp4). The wire sample whose surface was alloyed with Fe (cf. Figure 12) was used for the reaction with the $FeCl_3$ vapor.

the basis of the thermodynamic considerations given in Section 3, the Fe-Pt alloy showing ferromagnetism was unstable in $FeCl_3$ vapor. Thus, the results indicate that the reaction with $FeCl_3$ vapor under the coexistence of $FeCl_2$ cannot be used as the alloying and magnetizing treatment for Pt.

5. Conclusions

An $FeCl_x$ (x = 2, 3) vapor treatment that can effectively convert Pt into Fe-Pt alloy exhibiting ferromagnetism was examined using a combination of thermodynamic analyses and experiments. When reacted with $FeCl_2$ vapor at 1200 K for 1 h under the coexistence of metallic Fe, pure Pt samples were effectively alloyed with Fe, resulting in formation of the γ_2-FePt ferromagnetic phase. Thermodynamic considerations indicate that alloying of Pt proceeded mainly via the disproportionation of $FeCl_2$ vapor and that the gaseous phase containing $FeCl_x$ acted as a medium to transport Fe from the metallic Fe to the Pt samples. When the Pt sample alloyed with Fe was reacted with $FeCl_3$ vapor at 1200 K under the coexistence of $FeCl_2$, Fe was removed and the sample lost its magnetic property. It is therefore concluded that Pt can be effectively alloyed and magnetized by vapor treatment with $FeCl_2$, but it cannot be achieved using $FeCl_3$ vapor. The results obtained in this study indicate that alloying treatment with $FeCl_2$ vapor followed by magnetic separation has the potential to be a novel process that can effectively concentrate PGMs directly from catalyst scrap.

Acknowledgements

The authors are grateful to Dr. Kasuhiro Nose (The University of Tokyo, currently with JX Nippon Mining & Metals Corporation), Mr. Tetsuo Watanabe (The University of Tokyo, currently with Tanaka Kikinzoku Kogyo K. K.), Dr. Takanari Ouchi (Massachusetts Institute of Technology, currently with The University of Tokyo), Dr. Akihiro Yoshimura (Chiba University), and Mr. Ryohei Yagi (The University of Tokyo) for their valuable suggestions and comments. This research was financially supported by the Japan Society for the Promotion of Science (JSPS) through a Grant-in-Aid for Scientific Research (S) (KAKENHI Grant No. 26220910) and by the Mazda Foundation.

REFERENCES

1) F. Habashi (ed.): *Handbook of Extractive Metallurgy* (VCH Verlagsgesellschaft mbH, Weinheim, Germany, 1997) vol. III, pp. 1269–1326.
2) F. K. Crundwell, M. S. Moats, V. Ramachandran, T. G. Robinson, and W. G. Davenport: *Extractive Metallurgy of Nickel, Cobalt and Platinum-Group Metals* (Elsevier, Oxford, UK, 2011).
3) K. Nose and T.H. Okabe: in *Treatise on Process Metallurgy, Volume 3: Industrial Processes* (Elsevier, London, UK, 2013) pp. 1071–1097.
4) *PGM Market Report May 2016 Summary of Platinum Supply & Demand in 2015* (Johnson Matthey Plc., 2016) http://www.platinum.matthey.com/services/market-research/pgm-market-reports. Accessed 2016/5/26.
5) R. K. Mishra: Proceedings of the 17th International Precious Metals Conference (International Precious Metals Institute, 1993) 449–474.
6) H. Dong, J. Zhao, J. Chen, Y. Wu and B. Li: Int. J. Miner. Process. **145** (2015) 108–113.
7) F.L. Bernardis, R.A. Grant and D.C. Sherrington: React. Funct. Polym. **65** (2005) 205–217.
8) S. Suzuki, M. Ogino and T. Matsumoto: Journal of MMIJ **123** (2007) 734–736 (in Japanese).
9) M. Benson, C.R. Bennett, J.E. Harry, M.K. Patel and M. Cross: Resour. Conserv. Recycling **31** (2000) 1–7.
10) S. Owada, H. Seshimo, M. Miyashita, and K. Fujiwara: Proceedings of the 2nd International Symposium on East Asian Resources Recycling Technology (1993) 69–77.
11) S. Owada, Y. Tsubuku, and H. Nakayama: Proceedings of MMIJ Spring Meeting, (The Mining and Materials Processing Institute of Japan, 1994) 282–283 (in Japanese).
12) S. Owada and K. Shinoda: Proceedings of MMIJ Spring Meeting (The Mining and Materials Processing Institute of Japan, 2006) 69–70 (in Japanese).
13) W. Kim, B. Kim, D. Choi, T. Oki and S. Kim: J. Hazard. Mater. **183** (2010) 29–34.
14) G. Liu, T. Ichinose, A. Tokumaru and S. Owada: Mater. Trans. **55** (2015) 978–985.
15) G. Liu, A. Tokumura and S. Owada: Resources Processing **60** (2013) 28–35.
16) T. H. Okabe and J. Mitsui: Japan Patent, P5946034 (2016).
17) Y. Taninouchi, A. Suzue, and T. H. Okabe: Proceedings of 53rd Annual Conference of Metallurgists (COM 2014) (Canadian Institute of Mining, Metallurgy and Petroleum, 2014).
18) Y. Taninouchi, T. Watanabe and T.H. Okabe: Mater. Trans. **58** (2017) 410–419.
19) Y. Taninouchi, T. Watanabe and T.H. Okabe: Metall. Mater. Trans., B **48** (2017) 2027–2036.
20) Y. Taninouchi and Toru H. Okabe: in *Rare Metal Technology 2017* (Proceedings of the TMS 2017 Annual Meeting & Exhibition (TMS2017)), ed. by H. Kim, S. Alam, N. Neelameggham, H.

Oosterhof, T. Ouchi, X. Guan, (Springer, New York, 2017) pp. 119–127.
21) Y. Danzaki and T. Ashino: Anal. Sci. **17** (2001) 1011–1013.
22) I. Barin: *Thermochemical Data of Pure Substance, 3rd ed.*, (VCH Verlagsgesellschaft mbH, Weinheim, Germany, 1995).
23) P. Fredriksson and B. Sundman: Calphad **25** (2001) 535–548.
24) P. Franke and D. Neuschütz (eds.): *Binary systems. Part 3: Binary Systems from Cs-K to Mg-Zr*, (Springer Berlin Heidelberg, Germany, 2005).
25) P. Fredriksson and S. Seethraman: Scand. J. Metall. **30** (2001) 258–264.
26) H. Okamoto (ed.): *Phase Diagrams of Binary Iron Alloys*, (ASM International, Materials Park, Ohio, 1993) pp. 330–336.
27) K. Osaka, D. Sakaki and T. Takama: Jpn. J. Appl. Phys. **41** (2002) L155–L157.
28) Y. Nose, A. Kushida, T. Ikeda, H. Nakajima, K. Tanaka and H. Numakura: Mater. Trans. **44** (2003) 2723–2731.